Title

Trypanosoma brucei Translation Initiation Factor Homolog EIF4E6 Forms a Tripartite Cytosolic Complex with EIF4G5 and a Capping Enzyme Homolog

Journal

mSphere, 13(7)

ISSN

1556-6811

Authors

Freire, Eden R
Malvezzi, Amaranta M
Vashisht, Ajay A
et al.

Publication Date

2014-07-01

DOI

10.1128/ec.00071-14

Peer reviewed

EC
Journals.ASM.org

Trypanosoma brucei Translation Initiation Factor Homolog EIF4E6 Forms a Tripartite Cytosolic Complex with EIF4G5 and a Capping Enzyme Homolog

Eden R. Freire,[a] Amaranta M. Malvezzi,[a,d] Ajay A. Vashisht,[b] Joanna Zuberek,[c] Edwin A. Saada,[a] Gerasimos Langousis,[a] Janaína D. F. Nascimento,[d] Danielle Moura,[d] Edward Darzynkiewicz,[c,e] Kent Hill,[a] Osvaldo P. de Melo Neto,[d] James A. Wohlschlegel,[b] Nancy R. Sturm,[a] David A. Campbell[a]

Department of Microbiology, Immunology & Molecular Genetics, David Geffen School of Medicine, University of California at Los Angeles, Los Angeles, California, USA[a]; Department of Biological Chemistry, David Geffen School of Medicine, University of California at Los Angeles, Los Angeles, California, USA[b]; Division of Biophysics, Institute of Experimental Physics, Faculty of Physics, University of Warsaw, Warsaw, Poland[c]; Department of Microbiology, Centro de Pesquisas Aggeu Magalhães, Fundaçao Oswaldo Cruz, Recife, PE, Brazil[d]; Centre of New Technologies, University of Warsaw, Warsaw, Poland[e]

Trypanosomes lack the transcriptional control characteristic of the majority of eukaryotes that is mediated by gene-specific promoters in a one-gene–one-promoter arrangement. Rather, their genomes are transcribed in large polycistrons with no obvious functional linkage. Posttranscriptional regulation of gene expression must thus play a larger role in these organisms. The eIF4E homolog TbEIF4E6 binds mRNA cap analogs *in vitro* and is part of a complex *in vivo* that may fulfill such a role. Knockdown of TbEIF4E6 tagged with protein A-tobacco etch virus protease cleavage site-protein C to approximately 15% of the normal expression level resulted in viable cells that displayed a set of phenotypes linked to detachment of the flagellum from the length of the cell body, if not outright flagellum loss. While these cells appeared and behaved as normal under stationary liquid culture conditions, standard centrifugation resulted in a marked increase in flagellar detachment. Furthermore, the ability of TbEIF4E6-depleted cells to engage in social motility was reduced. The TbEIF4E6 protein forms a cytosolic complex containing a triad of proteins, including the eIF4G homolog TbEIF4G5 and a hypothetical protein of 70.3 kDa, referred to as TbG5-IP. The TbG5-IP analysis revealed two domains with predicted secondary structures conserved in mRNA capping enzymes: nucleoside triphosphate hydrolase and guanylyltransferase. These complex members have the potential for RNA interaction, either via the 5′ cap structure for TbEIF4E6 and TbG5-IP or through RNA-binding domains in TbEIF4G5. The associated proteins provide a signpost for future studies to determine how this complex affects capped RNA molecules.

The operon arrangement used by prokaryotes is an elegant solution to the question of regulated gene expression, with coordinated transcription of genes encoding enzymes within a given metabolic pathway under the control of a single promoter. In contrast, the majority of eukaryotes evolved independent promoters to control the expression of individual genes, and promoter types fall into classes that are activated or repressed in synchrony with functionally linked genes. Kinetoplastids employ an unusual blend of these two strategies, the constitutive transcription of polycistronic gene clusters that, apart from tandem gene arrays, typically show no discernible biochemical linkage within arrays (1, 2). The result is the virtual absence of genetic control at the level of gene transcription for mRNAs transcribed by RNA polymerase II (3, 4). *Trypanosoma brucei* has circumvented this limitation for the expression of a set of virulence factors associated with the variant surface glycoproteins. This family provides the coat on the cell surface and cycles a single member over time to allow this parasite to evade the host immune system. RNA polymerase I promoters provide temporal control to this gene set (5, 6). This unusual choice of polymerase is available to trypanosomes because of the mechanism that also provides a complex mRNA cap structure to all nuclear transcripts, namely, *trans* splicing of the spliced leader (SL) RNA (7).

The SL RNA is a small, independently transcribed molecule that is the source of the hypermethylated cap 4 structure that defines nucleus-derived mRNA in kinetoplastids (8). The cap 4 structure consists of cap 0 followed by 2′-*O*-methylation of the first four transcribed nucleotides and an additional three methylations on the first and fourth bases (9). The first 39 nucleotides are transferred by *trans* splicing to each gene transcript in a polycistronic array, which, coupled with 3′ polyadenylation (10), results in a monocistronic mRNA population looking very much like that from any other eukaryote with a few extra 5′ methylations. Other eukaryotes widely separated from each other in evolutionary terms use this combination of polycistronic transcription and *trans* splicing of their own flavor of SL (11–13).

RNA cap formation requires a minimum of three enzymatic activities, a triphosphatase to remove the gamma phosphate of the primary transcript, a guanylyltransferase to attach an inverted GTP cap via a triphosphate bridge, and a methyltransferase to complete the m^7G modification that defines cap 0 (14). This trio of activities is found in various combinations in different systems, including three separate proteins in yeast, a pairing of the first and second activities in metazoa and plants or the second and third

Received 17 March 2014 **Accepted** 12 May 2014
Published ahead of print 16 May 2014
Address correspondence to David A. Campbell, dc@ucla.edu.
Supplemental material for this article may be found at http://dx.doi.org/10.1128/EC.00071-14.

doi:10.1128/EC.00071-14

activities in kinetoplastids, and a single trifunctional enzyme in several viruses (14). In kinetoplastids the proteins adding cap 0 cotranscriptionally to the SL RNA are identified as TbCET1, a triphosphatase, and bifunctional TbCGM1, a guanylyltransferase and methyltransferase (15–17). Subsequent methylation of downstream nucleotides, referred to as cap 1, cap 2, and cap 4, can enhance translation levels (18).

The process of translation is more uniform in eukaryotes, requiring the recognition of a 5′ mRNA cap structure by an RNA cap-binding protein, eIF4E, a component of the eIF4F translation initiation complex. Entrance into the translation pathway could represent a key control point for polycistronically transcribing eukaryotes (19). In organisms with sophisticated mechanisms of transcriptional control such as humans, *Drosophila*, and yeast, the translation initiation machinery provides another level of control (20). The first step of translation initiation involves recognition of the mRNA cap by the eIF4F complex, which consists of eIF4E and the helicase eIF4A bound separately to a scaffold protein, eIF4G. Extended families of eIF4E and eIF4G proteins may result in an array of combinatorial possibilities for the modulation of translation (21). A minimal repertoire is found in the two model yeasts; *Saccharomyces cerevisiae* possesses one eIF4E and two eIF4Gs that have a functional overlap (22); *Schizosaccharomyces pombe* has two eIF4Es and one eIF4G that are distinguished during the stress response (23). Of the *trans*-splicing organisms, *Caenorhabditis elegans* has an extended family of five eIF4Es (24) and two eIF4G isoforms derived from alternative splicing (25). Four eIF4E homologs and five eIF4G homologs have been reported in *Leishmania* and *T. brucei* (26, 27), and the kinetoplastid-specific eIF4G binding partners have been identified for homologs eIF4E3 and eIF4E4 (28), with the eIF4E4 and eIF4G3 combination as the best candidates for the general translation initiation complex (28, 29). Ribosome profiling, the genome-wide analysis of mRNAs protected by the translation machinery, has demonstrated that translational regulation is an important component of regulated protein expression in *T. brucei* (30). The function of the other family members is unknown.

We have identified two further eIF4E family members in kinetoplastids, TbEIF4E5 and TbEIF4E6, focusing here on the molecular and cellular characterization of TbEIF4E6. Knockdown of TbEIF4E6 by RNA interference (RNAi) is linked with a phenotypic abnormality in flagellar attachment along the cell body of *T. brucei* and a notable reduction in social motility (SoMo) behavior. We have confirmed mRNA cap-binding activity for the protein, determined its TbEIF4G binding partner, and identified an intriguing copurifying hypothetical protein with domains predicted to function in mRNA cap 0 formation.

MATERIALS AND METHODS

Bioinformatics. The *T. brucei* eIF4E homolog TbE6 was identified by BLAST searches of the GeneDB database (31) by using the TbEIF4E5 sequence (Tb927.10.5020). Orthologs from *Leishmania tarentolae* and *Bodo saltans* were retrieved by BLAST searches of the TriTrypDB (32) and Wellcome Trust Sanger Institute (33) databases, respectively. Multiple-sequence alignments were performed with Clustal Omega (http://www.ebi.ac.uk/Tools/msa/clustalo/).

Plasmid construction. For the oligonucleotide primers used for amplification, see Table S1 in the supplemental material. Recombinant TbE6 was expressed from the p2171 plasmid. For interaction assays, the open reading frames of all eIF4E and eIF4G homologs were amplified by PCR and cloned into the yeast two-hybrid vectors pGAD and pGBK (Clontech Laboratories, Inc.). For conditional knockdown by RNAi, the TbE6 gene-internal fragments were amplified and cloned into the p2T7-177 vector (34). The 3′-terminal TbE6 gene fragments for carboxy-terminal epitope tagging of genes were PCR amplified, and the resulting fragments were cloned into the pC-PTP-Neo plasmid (35).

***In vitro* cap-binding assay.** Recombinant TbE6 protein tagged with His_6 was expressed in *Escherichia coli* Rosetta 2(DE3) cells. Expression was induced with 0.5 mM isopropyl-β-D-thiogalactopyranoside (IPTG) for 3 h at 37°C. Cells were harvested, disrupted by sonication, and centrifuged. The pellet was washed two times (20 mM HEPES-KOH [pH 7.2] 1 M guanidine hydrochloride, 2 mM dithiothreitol [DTT], 10% glycerol), and the inclusion bodies were dissolved in 50 mM HEPES-KOH (pH 7.2)–6 M guanidine hydrochloride–10% glycerol–2 mM DTT. Cell debris was removed by centrifugation (43,000 × *g* for 30 min). The protein (diluted to <0.1 mg/ml) was refolded by one-step dialysis against 50 mM HEPES-KOH (pH 7.2)–100 mM KCl–0.5 mM EDTA–2 mM DTT and purified by ion-exchange chromatography through a HiTrap SP column.

Time-synchronized fluorescence titrations were carried out on a PerkinElmer LS 55 Fluorescence Spectrometer at 20 ± 0.3°C (36) in 50 mM HEPES-KOH (pH 7.2)–100 mM KCl–0.5 mM EDTA–2 mM DTT. During the time course titration, 1-μl aliquots of cap analogue solutions were added to 1,400 μl of protein solution (0.1, 0.2, or 0.3 μM protein concentration). Changes in fluorescence intensity were measured at 325 or 340 nm with excitation at 280 nm and corrected for sample dilution and for inner-filter effects. Equilibrium association constants (K_{as}) were determined by fitting the theoretical curve of fluorescence intensity for the total cap analogue concentration to the experimental data points (36). The final K_{as} was calculated as a weighted average of three to five independent titrations. The fitting procedure used nonlinear least-squares regression analysis and was performed with Origin 6.0 (MicroCal Software).

***T. brucei* cell culture and RNAi.** YTAT procyclic *T. brucei* was grown at 27°C in SM medium (37) supplemented with 10% fetal bovine serum. Procyclic forms of *T. brucei* Lister 427 strain 29-13 were used for RNAi. Transfection was performed as described previously (38). Selection was performed with G418 (15 μg/ml), puromycin (10 μg/ml), or phleomycin (2.5 μg/ml), and clonal lines of selected cultures were obtained by limiting dilution in 96-well plates. To induce RNAi, 1 μg/ml tetracycline (Tet) was added to mid-log-phase cultures and growth was measured daily. Single-knockout, protein A-tobacco etch virus protease cleavage site-protein C (PTP)-tagged lines were constructed as described previously (35). To generate the $TbE6^{+/PTP}$ cell line, the 29-13 cell line was transfected with the plasmid cPTP-puro-TbE6, selected with puromycin, checked for PTP-tagged protein expression, transfected with the RNAi plasmid p2T7-177-TbE6, and then selected with phleomycin, generating the $TbE6^{+/PTP}$ RNAi cell line. PTP tagging of TbE6 to monitor knockdown in the 29-13 RNAi cell line affected one allele, leaving the second as the wild type (WT). For the genetic structure and validation of the cell lines, see Fig. S1 in the supplemental material.

Fluorescence microscopy. *T. brucei* cultures in mid-log phase (5×10^6 to 5×10^7 cells/ml) were used for immunofluorescence imaging as described previously (39). Aliquots of 1 ml were washed twice in 1 ml of phosphate-buffered saline (PBS), resuspended in 1 ml of PBS–0.01% paraformaldehyde, and incubated on ice for 5 min. The cells were centrifuged and resuspended in 0.5 ml of PBS. Approximately 20 μl of the cell suspension was spread on a microscope slide, dried at room temperature (RT), and then fixed at −20°C in acetone for 5 min and at −20°C in methanol for 5 min. The slides were dried at RT, and cells were rehydrated with 1 ml of PBS for 15 min and then blocked for 1.5 h at RT with blocking solution (PBS, 5% normal goat serum, 5% BSA). Blocked cells were incubated for 1.5 h in a rabbit anti-protein A antibody (Sigma) at 1:3,000 in blocking solution, washed 3× with PBS-T (PBS plus 0.05% Tween 20), incubated in 1:3,000 anti-rabbit IgG Alexa 488 (Invitrogen), washed three times with PBS-T and once with PBS, mounted on slides with Vectashield (Vector Laboratories) containing 4′,6-diamidino-2-phenylindole (DAPI), and viewed by fluorescence microscopy.

Metabolic labeling assay. [^{35}S]methionine incorporation was determined as described previously (27). RNAi-induced and uninduced TbE6$^{+/PTP}$ RNAi mid-log-phase cultures were centrifuged at 3,000 rpm at RT, washed once in methionine-free SM medium, and resuspended to a concentration of 1×10^7 cells/ml in methionine-free SM medium supplemented with 50 μCi/ml L-[*methyl*-^{35}S]methionine. After 1 h of incubation at 28°C, 50-μl aliquots were lysed (5 μl of 10% SDS, 2.5 μl of 1 M NaOH) and 10-μl volumes of these lysates were spotted in triplicate onto Whatman filter papers and dried at RT. The filters were then incubated on ice in 10% trichloroacetic acid (TCA) for 15 min and then boiled in 5% TCA for 10 min. After one methanol wash and one acetone wash, the filters were dried at RT. The radiolabel incorporated into proteins was measured with a Beckman LS 6500 Scintillation Counter. Experiments were performed three times in triplicate. The standard error was calculated and plotted in Microsoft Excel. Significance *P* values were calculated by one-way analysis of variance (ANOVA) (GraphPad Prism 5).

Flagellar attachment physical stress assay. WT and TbE6$^{+/PTP}$ RNAi cells with and without Tet were grown to mid-log phase. One-milliliter aliquots of primary culture were transferred to a microcentrifuge tube and subjected to 3,000 rpm in a desktop microcentrifuge (Eppendorf model 5415R) for 5 min at RT. The cell pellets were resuspended and washed twice in 1 ml of PBS with two additional 5-min spins at 3,000 rpm and then resuspended in 1 ml of PBS–10 μl of paraformaldehyde. An aliquot was spread on poly-L-lysine-treated coverslips and allowed to air dry before being mounted with coverslips and Vectashield (Vector Laboratories). Flagellar integrity was assessed by light microscopy at ×100 magnification. A total of 100 cells were scored for each of the three conditions, and the results were plotted with standard errors. Significance *P* values were calculated by one-way ANOVA (GraphPad Prism 5). A cell was scored as "detached" if the flagellum was looped away from the cell body, separated from part or all of the cell body, or absent altogether.

Sedimentation assay. Motility in a liquid environment was quantified by spectrophotometry similar to what was described elsewhere (40). Cells with integrated RNAi constructions were incubated with or without Tet for 72 h and then resuspended at 5×10^6/ml in fresh medium with or without the drug. Six replicates (1 ml) were transferred to cuvettes and incubated without shaking under standard conditions. The optical density at 600 nm (OD_{600}) was measured in triplicate every 8 h, with three cuvettes left undisturbed to measure sedimentation and three cuvettes mixed prior to measurement. The ΔOD_{600} of each sample was calculated by dividing the OD_{600} of the resuspended samples by those of the undisturbed samples.

SoMo assays. SoMo assays on semisolid agarose plates were performed as described previously (41). Plates contained either methanol (diluent) or Tet (final concentration, 1 μg/ml) for the "minus-Tet" and "plus-Tet" conditions, respectively. The plates were inoculated with 5.5 μl of cells from suspension cultures at approximately 1.0×10^7 cells/ml. The plus-Tet cells were induced for 72 h prior to plating. Following inoculation, the plates were closed, left to sit for 20 min, sealed with Parafilm, and then incubated at 27°C with 5% CO_2. Plates were photographed at 120 h with a white light box and a velvet cloth to provide background contrast. Images were acquired with a Pentax Optio M30 camera and cropped in Adobe Photoshop.

Yeast-two hybrid assays. Yeast strain PJ69-4A was cultivated overnight at 30°C in YPD medium (42). Each transformation used 1 ml of a cell suspension washed and resuspended in 100 μl of Tris-EDTA (TE)–100 mM lithium acetate buffer and incubated at RT for 15 min. The cells were centrifuged and resuspended in 360 μl of transformation buffer (1× TE, 1 mM lithium acetate, 50% PEG 8000, 2 mg/ml boiled salmon sperm DNA), simultaneously transformed with GBK (Tryp$^+$) and GAD (Leu$^+$) plasmids expressing individual *T. brucei* 4E and 4G homologs, and incubated for 30 min at RT. Subsequently, the cells were incubated at 42°C for 20 min and then centrifuged. The pellet was resuspended in 2 ml of dropout medium (minimal medium minus tryptophan and leucine) and incubated overnight at 30°C. After dropout incubation, the OD_{600} was checked and all of the cultures were centrifuged, diluted to an OD_{600} of 0.5 in dropout medium (minimal medium minus tryptophan, leucine, and histidine), plated on solid dropout medium containing 3-amino-1,2,4-triazole (3AT) in serial dilutions, and incubated at 30°C for 5 days. The positive-control plates used plasmids pGADT7-T and pGBKT7-53 (Clontech Laboratories Inc.) for transformation.

Native gel electrophoresis. Blue native gel analysis was performed as described previously (43). Samples were prepared as follows: Mid-log-phase culture cells were washed twice in PBS, resuspended in 24 μl of extraction buffer (25 mM HEPES, 150 mM sucrose, 20 mM potassium glutamate, 3 mM $MgCl_2$, 0.5% NP-40, 150 mM KCl, 0.5 mM DTT, Sigma*FAST* EDTA-free protease inhibitor cocktail [Sigma-Aldrich]), incubated on ice for 20 min, and centrifuged at full speed for 10 min at 4°C. Eighteen microliters of the supernatant was added to 6.25 μl of 4× native PAGE buffer and 1 μl of G-250 Coomassie sample buffer. The samples were electrophoresed through precast 4 to 16% native PAGE Novex Bis-Tris gels in accordance with the manufacturer's specifications (Life Technologies). The NativeMark unstained protein standard (Life Technologies) was used to estimate complex sizes. Proteins were transferred to 0.2-μm Immun-Blot polyvinylidene difluoride membranes (Bio-Rad). Membranes were fixed in 8% acetic acid for 15 min, rinsed with water, and incubated with a primary or secondary antibody. The size marker lane was removed prior to antibody incubation, air dried, equilibrated with methanol, and stained with Coomassie dye for visualization.

Tandem affinity purification. Purification was performed with 500 ml of culture (5×10^6 cell/ml). For tandem affinity purification, the PTP tag was used and purification was performed as described previously (35). The total elution from the protein C column was either (i) resolved by SDS-PAGE and visualized by silver staining (Bio-Rad Silver Staining plus) or (ii) TCA precipitated and subjected to multidimensional protein identification technology (MudPIT) mass spectrometry.

MudPIT. The TCA-precipitated proteins were digested by trypsin and subjected to mass spectrometry as described previously (44). The proteomic data were analyzed by using the SEQUEST and DTASelect2 algorithms against the *T. brucei* genome database (1), filtering by a peptide-level false-positivity rate of 5%, and a minimum of two peptides per protein (45).

RESULTS

Two new members of the kinetoplastid eIF4E homolog family. The dearth of transcriptional control in trypanosomes means that the organism must rely on downstream control mechanisms to modulate levels of gene expression. Therefore, mRNA is an attractive target for regulation and we chose to search for cap-binding proteins that could mediate recognition of transcripts in general or perhaps of specific subgroups of messages. Reexamination of the GeneDB database with eIF4E family members from baker's yeast revealed a new protein, Tb927.10.5020, that we duly named TbEIF4E5 and refer to here as TbE5. A reciprocal BLAST search with the TbE5 sequence revealed a further related protein, Tb927.7.1670, that we designated TbEIF4E6 (TbE6). Here we present the functional characterization of TbE6.

Both TbE5 and TbE6 carry the hallmarks of the IF4E superfamily core domain, including motifs required for RNA cap binding and for eIF4G protein interaction (Fig. 1; see Table S2 in the supplemental material). Atypically, both cap-binding pi-pi sandwich residues showed a conservative replacement of tryptophan (W) with phenylalanine (F). Replacement of W73 with a nonconservative ring-containing histidine (H) was found in the eIF4G interaction domain. Both proteins have orthologs in all *Leishmania* species, as exemplified here by *L. tarentolae*, and in the distantly related parabodonid *B. saltans* (see Fig. S2A in the supplemental material). An additional conserved block spanning 7 of 13 amino

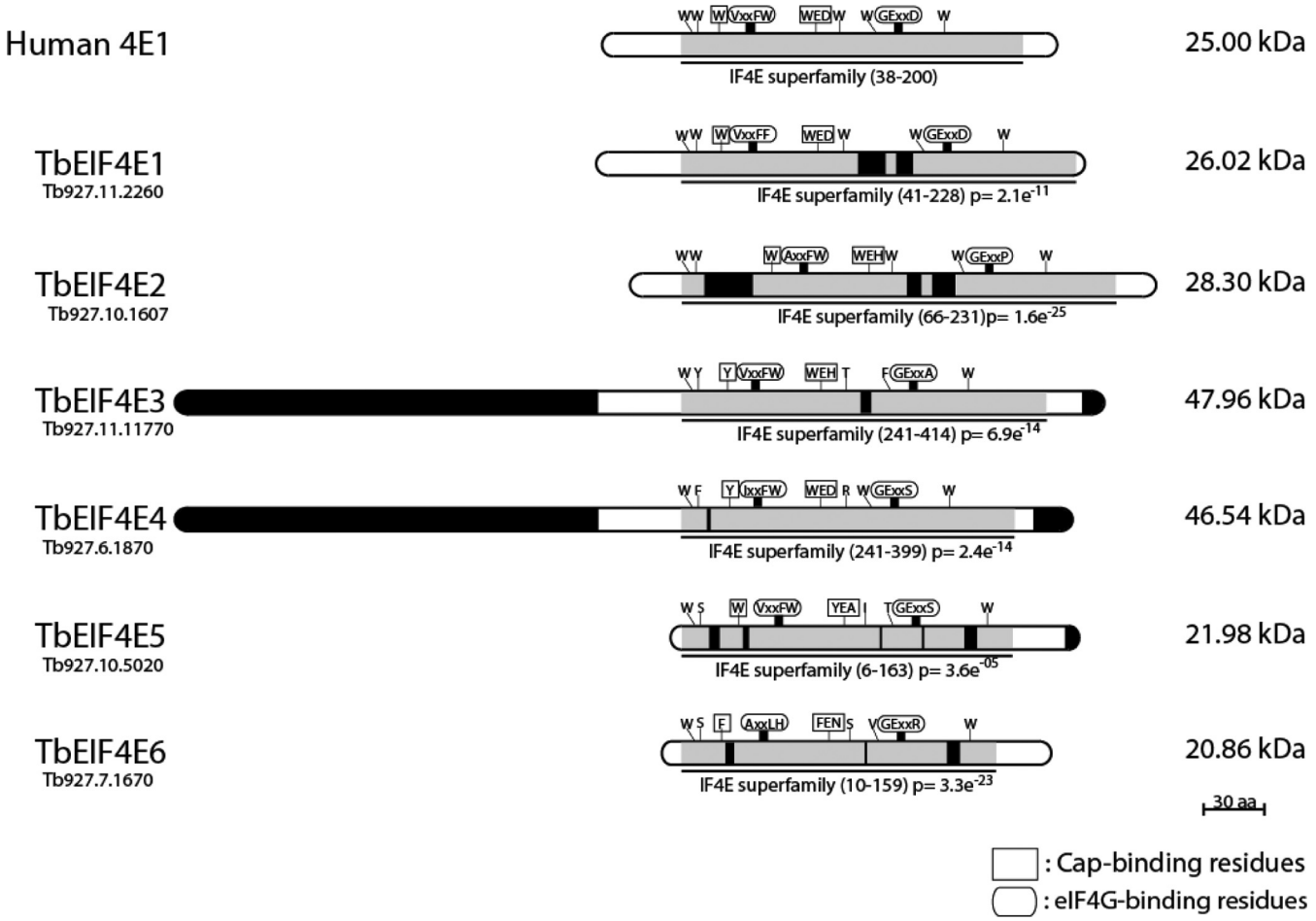

FIG 1 The key domains and motifs of the *T. brucei* and human eIF4E homologs are conserved. This comprehensive diagram aligns the IF4E superfamily domains of the six proteins and highlights nucleotides and motifs critical for RNA cap binding. Highlights include the conservation of the family domain (gray) with *P* values indicated, insertions (black), and the amino acids involved in cap binding (in squares) and eIF4G binding (in elongated circles).

acids (aa) was observed in the short NH-terminal domain. The conservation of TbE6 eIF4E-like homologs suggests a common role in kinetoplastid biology.

TbE6 binds cap analogs *in vitro*. To determine if TbE6 could bind mRNA cap structures, we measured the efficiency of recombinant TbE6 binding to four cap analogs *in vitro*. The hypermethylated SL RNA cap equivalent was represented by cap 4, while the standard cap 0 structure binding was tested with the m^7GTP and m^7GpppA substrates. GTP served as a control not expected to interact with a cap-binding protein. The fluorescence titrations carried out for the four analogs revealed poor binding of TbE6 to the m^7GpppA analog, with a K_{as} similar to that observed for LeishIFE-1, LeishIFE-2, and LeishIFe-3, and better binding to m^7GTP with a K_{as} of $0.16 \pm 0.1\ \mu M^{-1}$ and the cap 4 analog with a K_{as} of $0.16 \pm 0.2\ \mu M^{-1}$ (Fig. 2). Relative to *Leishmania* (26), TbE6 bound m^7GTP with an affinity identical to that of LeishIFE-1 and bound cap 4 with an affinity between those of LeishIFE-3 and LeishIFE-1.

The relatively low levels of cap recognition relative to the isolated mouse protein may reflect a requirement for other structural elements, such as eIF4G or an RNA chain, to facilitate RNA binding (46–49).

TbE6 is cytosolic. The four kinetoplastid eIF4E protein family

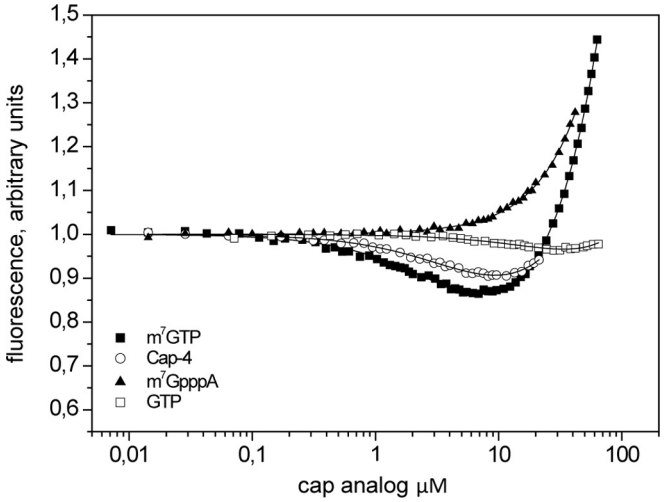

FIG 2 Cap-binding activity of recombinant TbE6. The fluorescence titration curves with four cap analogs were determined by TbE6 fluorescence quenching observed at 325 nm. Protein fluorescence was excited at 280 nm. The trypanosome WT mRNA cap is hypermethylated Cap-4, and the typical eukaryotic cap structure is represented by both the m^7GTP and m^7GpppA cap 0 analogs. Nonmethylated GTP is a negative control for cap 0-specific binding.

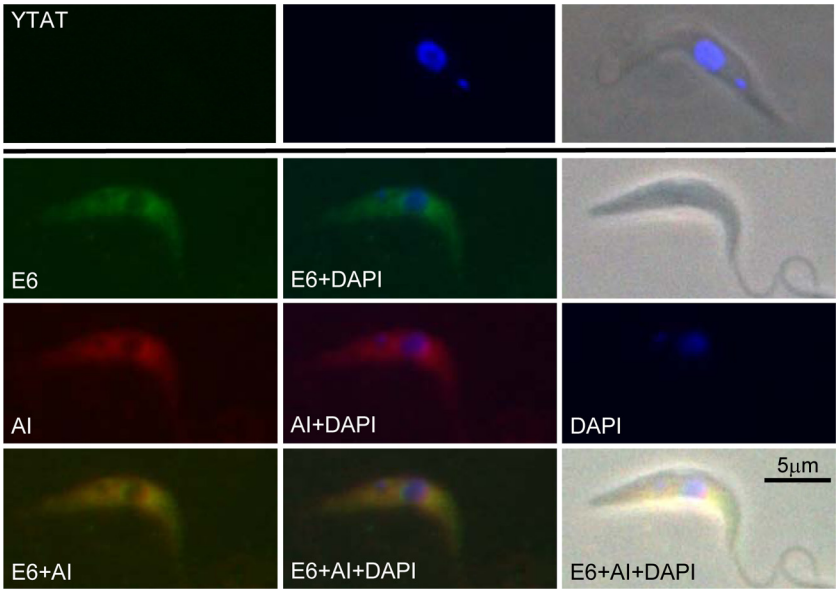

FIG 3 TbE6 is cytosolic. The subcellular localization of TbE6 in *T. brucei* procyclic cells was determined by IFA analysis with an anti-protein A antibody that recognized the TbE6-PTP fusion protein epitope tag (green). The positive control for cytosolic location was counterstaining with a rabbit antibody against the TbEIF4AI protein (red) (51). The outline of the cell is indicated in the phase-contrast image. The negative control was nontransfected control YTAT cells. Nuclear and kinetoplast DNAs were visualized by DAPI staining.

members either localize to the cytosol or are present in both the nucleus and the cytosol (27, 50). To assess function, the TbE6 protein was localized and assayed for its requirement in procyclic cell viability under normal culture conditions. The absence of strong antibodies to our target protein and the availability of excellent epitope-tagging systems prompted us to generate an epitope (PTP)-tagged gene line lacking the endogenous WT gene, TbE6$^{-/PTP}$ (see Fig. S1A in the supplemental material).

Immunolocalization of the TbE6$^{-/PTP}$ protein with the PTP tag revealed a diffuse cytosolic distribution and majority exclusion from the nucleus (Fig. 3), similar to TbE3 and TbE4 (27, 50). As a cytosolic localization control, the slide was counterstained with an antibody recognizing TbEIF4AI (51). The kinetoplast and nuclear DNAs were stained with DAPI.

To facilitate the monitoring of RNAi knockdown of the TbE6 protein, we used a TbE6$^{+/PTP}$ RNAi cell line (see Fig. S1B in the supplemental material) for our assays. RNAi against the TbE6 transcript resulted in the reduction of epitope-tagged TbE6 levels to approximately 12.5% of the uninduced levels by day 3 (see Fig. S3A). A minor difference in the growth rate compared to that of the WT was detected in our lines (Fig. 4A). This result suggests that TbE6 is not essential for WT cell division; however, the result is contrary to those obtained in the high-throughput RNAi analysis conducted by Alsford et al., which indicates that TbE6 is essential for normal growth (52). To provide ample time for the RNAi effect to be seen, we extended the analysis for 15 days and saw no relative change in culture growth despite continued knockdown of TbE6 protein levels (see Fig. S3B). The relative efficiency of the knockdown may explain the discrepancy, if an approximately 12.5% level of TbE6 is sufficient for viability.

To test TbE6 for a role in general translation, we quantitated the effect of RNAi knockdown on protein synthesis. RNAi cells at days 4 and 7 postinduction were metabolically labeled with [^{35}S]methionine (Fig. 4B). The isotope incorporation levels of

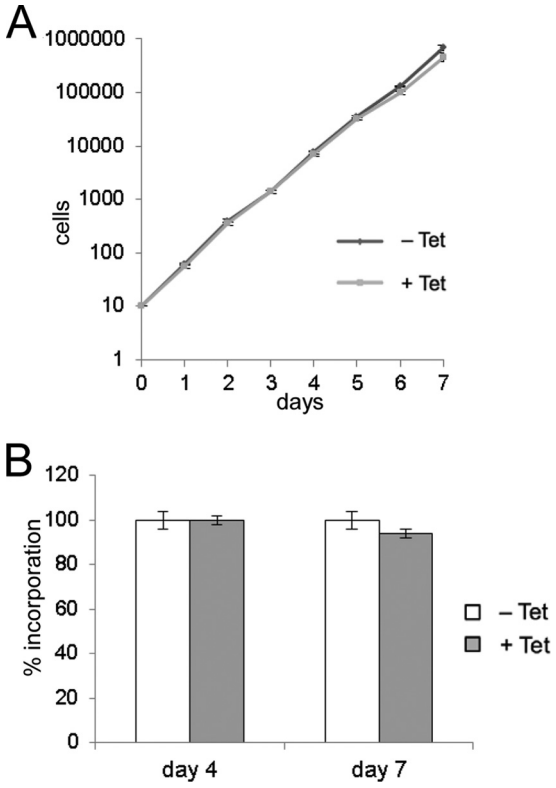

FIG 4 The TbE6 protein does not have a primary role in translation. (A) Growth curve for triplicate RNAi knockdowns of TbE6 in procyclic cells marked with standard errors. Induced TbE6$^{+/PTP}$ RNAi cultures (+ Tet) are compared to uninduced (− Tet) TbE6$^{+/PTP}$ RNAi cells. (B) [^{35}S]methionine metabolic labeling of cultures induced for TbE5 RNAi knockdown at 4 and 7 days postinduction compared to that of noninduced cultures.

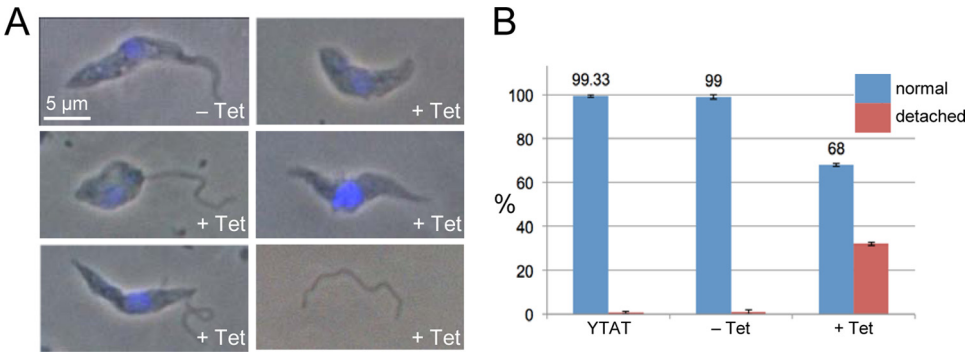

FIG 5 Knockdown of TbE6 results in flagellar detachment upon manipulation. (A) Phase-contrast microscopy of cells left uninduced or induced for RNAi against TbE6. DNA was visualized by counterstaining with DAPI. The cells were prepared for IFA analysis of TbE6-PTP. Flagella detached from the cell body are shown below the minus-Tet control panel; absent or free flagella are shown to the right. (B) Histogram showing the integrity of flagellar attachment along the length of the cell body as measured after benchtop centrifugation, including standard errors. WT (YTAT) and uninduced TbE6$^{+/PTP}$ RNAi cells were compared with induced TbE6$^{+/PTP}$ RNAi cells.

both uninduced and induced cultures were comparable on day 4; by day 7, the ^{35}S levels in the induced cultures were 6% lower than those in the uninduced lines. The nonsignificant reduction (P = 0.2375) of methionine incorporation in the presence of approximately 85% reduced TbE6 levels indicates that TbE6 does not have a primary role in general translation initiation. We cannot definitively rule out a scenario in which approximately 12.5% of the WT TbE6 level is sufficient for a normal level of translation.

Because of the survivorship of the cultures, we attempted to create a genetic TbE6 knockout line by eliminating both endogenous alleles. Three failed attempts to remove the second TbE6 allele (data not shown) suggested that the protein is indeed essential for the survival of procyclic cells. The behavior of our RNAi inductions relative to the study of Alsford et al. could be due to a variety of factors, including the relative efficacy of knockdown, the integration site, the vector choice, and/or the presence of the PTP tag on the protein. Alternative approaches using knockout lines in combination with inducible copies of the TbE6 gene (53, 54) or RNAi targeting of the PTP tag (55) are being explored to resolve the issue.

Knockdown of the TbE6 protein affects motility and the stability of flagellar attachment. The survivorship of our RNAi line provided an opportunity to examine the function of TbE6. While pursuing our analysis of TbE6 under RNAi induction conditions, we noted a difference in the morphology of induced cells.

On slides fixed for indirect immunofluorescence assay (IFA) analysis, cells grown in the presence of Tet had a high proportion of abnormal flagellar phenotypes. Specifically, their flagella were detached from the length of the cell body or in many cases completely absent and visible in isolation on a slide (Fig. 5A). Flagellar detachment was not evident in live cultures or cultures diluted for counting in a Neubauer chamber and appeared to be dependent on forces such as those experienced during centrifugation and resuspension. To follow up on this observation, we devised a physical-stress assay. Induced TbE6 RNAi cells were centrifuged for 5 min at 3,000 rpm, the standard conditions used to pellet *T. brucei* cells from culture. By counting a total of approximately 100 cells by light microscopy, we assessed the percentage of detached flagella. Over 30% of the induced cells showed various levels of flagellar detachment or loss after this treatment (Fig. 5B). In uninduced and WT cells, flagella were largely intact under all of the conditions tested. Thus, a decrease (P = <0.001) in flagellar attachment strength is manifest with the reduction of TbE6.

The potential for impaired motility due to this fragile condition was gauged via a sedimentation assay to assess the ability of induced cells to remain in suspension in liquid media. Induced and uninduced cultures were placed in pairs of spectrophotometer cuvettes, and OD_{600} was measured at various time points. A control cuvette was shaken prior to measurement and compared with its unshaken counterpart. Comparison of WT YTAT cells with uninduced and induced TbE6 RNAi cultures revealed no difference (P = 0.1612) in cell settling (Fig. 6A); thus, basic motility appeared normal. Next, the ability of TbE6-depleted cells to participate in SoMo behavior was examined by assessing the formation of projections along semisolid surfaces (41). This assay revealed a significant difference (P = 0.0032). Uninduced cells showed 100% SoMo (17/17) with a mean of 8.59 ± 1.06 projections per plate, while RNAi-induced cells showed 44.4% SoMo (8/18 plates) with a mean of 3 ± 1 projections per plate (Fig. 6B and C; see Fig. S4 in the supplemental material). While the RNAi-induced cells produced significantly fewer projections, the cells themselves were viable and continued to divide at the point of inoculation.

TbE6 binds the TbG5 homolog. Translation initiation is mediated by a three-component complex in which eIF4G acts as a scaffold for interactions with eIF4A and eIF4E (56). In trypanosomes, the six eIF4E proteins have a selection of five known eIF4G homologs to choose from and, in addition to Leish4E-IP (57), likely a cohort of as-yet-unknown partners. To determine which, if any, of the TbEIF4G homologs interact with TbE6, each potential pairing was tested individually in a heterologous system.

The yeast two-hybrid assay detects interactions between two proteins, termed "bait" and "prey," as indicated by the activation of a promoter in the yeast cells that permits growth. In this assay, yeast growth in the presence of 5.0 mM 3AT indicates a strong interaction. By placing our proteins of interest in "bait" and "prey" positions, we tested potential interactions for our five possible combinations (Fig. 7A). TbE6 paired exclusively with TbEIF4G5 (TbG5; 84.6 kDa; Tb927.8.4500), an essential protein in the procyclic stage, according to the Alsford RNAi study (52), and showed no interaction with any of the other TbEIF4G family members (see Fig. S5 in the supplemental material).

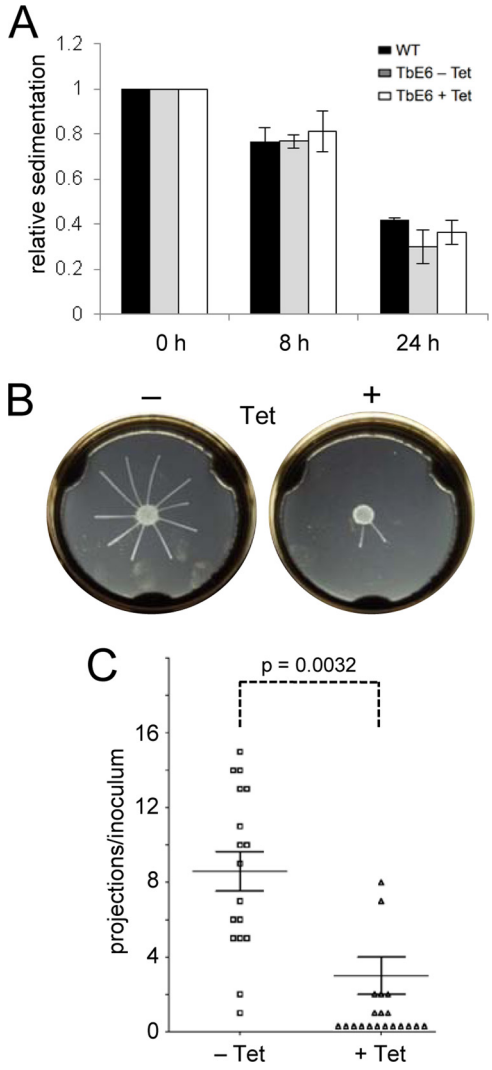

FIG 6 TbE6 depletion does not affect motility in liquid culture but results in reduced SoMo. (A) Turbidity assay measuring cell sedimentation in stationary cuvettes. Standard error bars were derived from experiments performed in triplicate for 0-, 8-, and 24-h samples. (B) SoMo assessment under TbE6 RNAi knockdown conditions. Representative semisoft agarose plate SoMo assays of uninduced or induced cells incubated for 5 days postinoculation are shown. Cell mass projections were scored as a measurement of SoMo, with 10 and 2 projections scored on the minus-Tet and plus-Tet sample plates, respectively. (C) Graphic summary of the TbE6 SoMo assay indicating means and standard errors for 17 control and 18 induction plates. Each point represents the number of radial projections from the site of inoculation. *P* values were determined by unpaired two-tailed *t* tests.

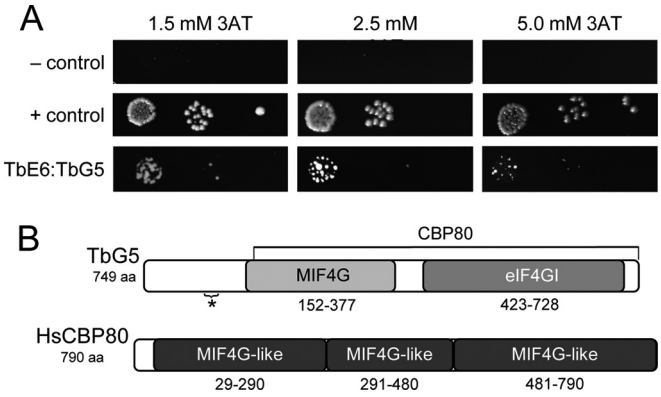

FIG 7 Direct interaction of TbE6 with TbG5. (A) Yeast-two-hybrid assay used to detect any interactions between TbE6 and the five Tb4G homologs in the presence of three concentrations of 3AT to vary the stringency of the interaction. For the full panel tested, see Fig. S5 in the supplemental material. The positive interaction is shown here with the controls. The positive control was a combination of pGADT7-T and pGBKT7-53; the negative control contained the empty vectors. Interaction strength is inferred by colony size as follows: ≥2 mm, strong; 1 to 2 mm, moderate; ≤1 mm, weak. (B) Structural domains protein identified by PHYRE[2] in the TbG5. In TbG5, the asterisk denotes a low-confidence HMG box (70), a possible nucleic acid binding site. MIF4G/DAP5, middle of 4G/death-associated protein (61); eIF4GI, human isoform I (71).

TbG5 carries three domains with potential nucleic acid interaction potential (Fig. 7B). Starting from the amino terminus, PHYRE[2] examination revealed an ~20-aa stretch with general similarity to DNA-binding α-helical structures (high-mobility group [HMG] box; 36 to 52% confidence), followed by a central midle-of-eIF4G (MIF4G) domain (100% confidence) and ending with an eIF4GI-like domain (98.4% confidence). Both of the high-confidence domains showed a match to human nuclear cap-binding complex subunit CBP80 (94.5% confidence) encompassing the C-terminal HEAT2 and HEAT3 domains (a repeat found in Huntingtin, elongation factor 3, protein phosphatase 2A, and TOR1 proteins) (58), an interesting hit since a CBP80 homolog was not found in the *T. brucei* nuclear cap-binding complex (59).

The exclusivity of the interaction of TbE6 with TbG5 is an indication that specific functions are associated with different family members. The TbG5 protein contains several suggestive domains, including a predicted HMG box for nucleic acid binding in the amino-terminal domain and a MIF4G domain similar to those found in the related proteins cwc22 and dap5, which are involved in exon junction complex assembly and internal ribosome entry site-mediated translation (60, 61). Thus, TbG5 may carry two regions with RNA selection potential. The incorporation of other proteins or RNAs into the equation may shed light on the function of the TbE6 complex.

TbE6 is a member of a protein complex. Our yeast two-hybrid interaction assays indicate that TbE6 associates with the TbG5 homolog, and validation of their binding in *T. brucei* with each other and with other proteins was examined by monitoring the sizes of complexes containing tagged proteins first by blue native gel electrophoresis and then by MudPIT mass spectroscopy analysis of individual components in tandem affinity-purified complexes.

To validate that TbE6 was in a high-molecular-mass complex and to estimate the size(s) of the protein complex(es), extracts of TbE6$^{-/PTP}$ were visualized by blue native gel analysis and Western blotting with anti-protein A antibody. The analysis of ~41-kDa PTP-tagged TbE6 revealed a major band migrating between the 242- and 480-kDa markers at ~300 kDa and a minor band between the 66- and 146-kDa markers migrating at ~90 kDa (Fig. 8). A high-molecular-mass complex at ~300 kDa containing ~104-kDa TbG5-PTP was detected in a TbG5$^{-/PTP}$ line (see Fig. S1 in the supplemental material). The ~90-kDa TbE6-containing band was not detected in the TbG5-PTP sample and may represent free TbE6-PTP or a subcomplex not containing TbG5.

The combined data from these experiments are consistent with

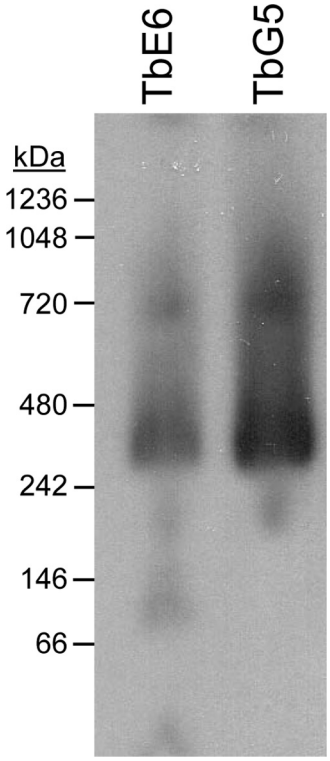

FIG 8 TbE6 migration supports interaction with a high-molecular-mass complex. Blue native gel electrophoresis of cell extracts from TbE6-PTP- and TbG5-PTP-transfected *T. brucei*. Lysates were transferred to nitrocellulose membranes and probed with an antibody directed against the protein A domain of the PTP tag of TbE6 and TbG5.

the formation of the predicted Tb4E/Tb4G complex *in vivo* and suggest the presence of additional components in the complexes formed by both proteins.

A protein with mRNA capping domains copurifies with TbE6. To isolate the specific complexes and identify their constituents, the TbE6$^{-/PTP}$ line was used for tandem affinity complex purification with subsequent protein identification by MudPIT. Purifications were performed a minimum of three times with various levels of elution stringency, and the products were subjected to tryptic digestion and analyzed by tandem mass spectrometry. Two peptide hits are required for the validated identification of a given protein. A limitation of this procedure is an inability to identify peptides that carry modifications that alter their mass, since the *in silico* values generated from GeneDB are based on pure amino acid weights.

Two proteins similar in peptide coverage consistently associated with TbE6 (Table 1). In agreement with the TbE6-TbG5 yeast two-hybrid result, TbG5 scored strongly in the TbE6-PTP purifications. The third hit was a protein of 70.3 kDa (Tb927.11.14590) annotated as "hypothetical" that was scored as essential for procyclics and the other three life stages assayed by RNAi (52) and is referred to here as TbG5-IP (TbG5-interacting protein). Both TbG5 and TbG5-IP are well conserved in kinetoplastid protozoa (see Fig. S2B and C in the supplemental material). Confirmation of the interaction of this trio and elimination of the purification-specific background were accomplished by performing PTP purifications from tagged TbG5 and TbG5-IP cell lines (see Fig. S1C and D). Consistent with the blue native gel migration, TbE6 copurified with TbG5-PTP; the TbG5-IP abundance score was >85% of that of TbG5-PTP itself, compared to ~33% relative abundance for TbE6 in this purification (Table 2). Likewise, TbG5-IP-PTP MudPIT analysis yielded itself, TbG5, and TbE6 in order of decreasing abundance, with the fourth hit present at 25% of the level of TbE6 (Table 3). Considering the top 20 proteins identified in each of the three purifications (11 to 20 are not shown), 2 additional proteins are common to all three analyses, a paraflagellar rod component protein (Tb927.10.11300) and a voltage-dependent anion-selective channel protein (Tb927.2.2510). Taken together, these data are indicative of a primary interaction between TbG5 and the TbG5-IP hypothetical protein, with a strong association of that pair and the TbE6 protein. This is reminiscent of eIF4G acting as a scaffold that brings accessory proteins to eIF4E once it has captured a capped RNA.

To determine the target of physical interaction of TbG5-IP within the TbE6 complex, a yeast two-hybrid assay was used to test the potential for direct binding with TbE6 or TbG5. The TbG5 protein bound to the 70.3-kDa TbG5-IP protein in both the bait and prey configurations, while both TbE6 trials were negative for yeast growth (Fig. 9A), indicating that TbG5 is the scaffold for both TbE6 and TbG5-IP. Localization of TbG5-IP-PTP was performed with the protein C antibody to visualize the target. The staining pattern indicated a cytosolic localization for this third complex member (Fig. 9B), mirroring the distribution seen for

TABLE 1 Proteins copurifying with TbE6-PTP in three different purifications identified by MudPIT

Gene product	GeneDB identifier[a]	Molecular mass (kDa)	AvUniPepts[b]	% Coverage	NSAF[c]
TbEIF4E6	Tb927.7.1670	20.90	19	54.30	45,527.06
TbEIF4G5	Tb927.8.4500	84.60	50	46.30	14,270.11
Hypothetical protein	Tb927.11.14590	70.30	20	29.60	2,606.34
Paraflagellar rod component	Tb927.10.11300	14.32	5	27.00	1,434.29
Hypothetical protein	Tb927.5.2260	12.40	3	23.90	1,204.16
Glycerol-3-phosphate dehydrogenase	Tb927.8.3530	37.80	8	23.20	911.62
Cytochrome oxidase V	Tb927.9.3170	22.23	2	9.70	790.32
Hypothetical protein	Tb927.4.2740	16.32	4	30.00	774.52
EF1b	Tb927.4.3590	24.30	4	22.60	544.04
Triosephosphate isomerase	Tb927.11.5520	26.81	5	25.20	516.34

[a] GeneDB identifiers are from *T. brucei* 927, version 6.0 (www.genedb.org and www.tritrypdb.org). Temporary GeneDB identifiers retrieved from peptide analysis based on *T. brucei* 927 version 2.2: Tb927.11.14590, Tb11.01.6200; Tb927.9.3170, Tb09.160.1820; Tb927.11.5520, Tb11.02.3210.
[b] AvUniPepts, number of peptides identified.
[c] NSAF, normalized spectral abundance factor.

TABLE 2 MudPIT identification of proteins copurifying with TbG5-PTP

Gene product	GeneDB identifier[a]	Molecular mass (kDa)	AvUniPepts[b]	% Coverage	NSAF[c]
TbEIF4G5	Tb927.8.4500	84.60	60	56.10	12,149.62
Hypothetical protein TbG5-IP	Tb927.11.14590	70.30	34	44.40	10,487.22
TbEIF4E6	Tb927.7.1670	20.90	8	22.00	3,979.55
Voltage-dependent anion channel	Tb927.2.2510	29.19	12	49.60	3,507.47
Histone H3	Tb927.1.2470	14.80	4	32.30	2,373.47
Histone H2A	Tb927.7.2900	14.20	2	14.20	1,056.03
UMSBP	Tb927.10.6070	14.60	6	37.90	544.26
UMSBP	Tb927.10.6060	21.83	7	27.70	408.84
ALBA3	Tb927.4.2040	20.80	5	33.20	343.75
Cyclophilin A	Tb927.11.880	18.71	3	14.10	307.49

[a] GeneDB identifiers are from *T. brucei* 927, version 6.0 (www.genedb.org and www.tritrypdb.org). Temporary GeneDB identifiers retrieved from peptide analysis based on *T. brucei* 927 version 2.2: Tb927.11.14590, Tb11.01.6200; Tb927.11.880, Tb11.03.0250.
[b] AvUniPepts, number of peptides identified.
[c] NSAF = normalized spectral abundance factor.

TbE6-PTP and the cytosolic control TbEIF4AI. Examination of the migration of TbG5-IP-PTP in the blue native gel system revealed a broad band whose front migrated faster than the 242-kDa marker and the TbE6 and TbG5 complexes but tailed into an overlap with the other bands (Fig. 9C).

Bioinformatic analysis of TbG5-IP by PHYRE^2 (62) revealed two provocative domains associated with mRNA 5′ cap formation (Fig. 10A). The amino half of TbG5-IP displayed similarity to nucleoside triphosphate (NTP) hydrolase secondary structure (99.1% confidence), a broad domain that includes the triphosphatase enzymes involved in the first step in cap 0 formation on primary transcripts. The carboxyl half of the protein consisted almost entirely of a guanylyltransferase domain (99.8% confidence). Adjacent to the gene for TbG5-IP (Tb927.11.14590) on chromosome 11 is a gene for a protein (Tb927.11.14580) identified previously on the basis of guanylyltransferase activity named capping enzyme 1 or TbCE1 (63). TbCE1 has the same domains as TbG5-IP, each with 100% confidence as ascribed by PHYRE^2, and differs primarily through the NH-terminal extension on TbG5-IP. The high level of sequence similarity indicates that these genetic neighbors arose through a duplication event in the genome. TbCE1 is not thought to perform the cap 0 addition on the SL RNA, as that task is ascribed to the triphosphatase TbCET1 (15) and the bifunctional guanylyltransferase TbCGM1 (16, 17).

The TbE6 complex contains three consistent members, each of which purifies the other two in PTP and MudPIT analyses, with TbG5 serving as a scaffold between TbE6 and TbG5-IP (Fig. 10B). The predicted size of this complex is 194.7 kDa when including a PTP tag, somewhat smaller than the ~300 kDa indicated by blue native gel analysis of TbE6 and TbG5 (Fig. 8) but more consistent with the analysis of TbG5-IP (Fig. 9C). The complex may be dynamic with respect to protein composition, causing the apparent anomalies in migration. Other variables that could affect migration through this nondenaturing gel system include proteins that may remain in association with the PTP-tagged complex in the blue native system but are lost upon affinity purification. In nondenaturing gels, the size of the complex is unlikely to reflect the additive molecular mass of its components because of the effects of quaternary structure.

The functional domains carried by TbG5-IP indicate that this complex has a role in the modulation of gene expression through the modification of mRNA 5′ ends. Coupled with the observation of compromised flagellar attachment upon TbE6 depletion and the general cytosolic distribution of the three proteins identified, this complex may represent a gateway for the expression of proteins involved in flagellar attachment to the cell body either directly or secondarily.

DISCUSSION

Posttranscriptional mechanisms of control in organisms such as trypanosomes that lack specific transcriptional modulation for the vast majority of their genes must play a key role in gene ex-

TABLE 3 MudPIT identification of proteins copurifying with TbG5-IP-PTP

Gene product	GeneDB identifier[a]	Molecular mass (kDa)	AvUniPepts[b]	% Coverage	NSAF[c]
Hypothetical protein TbG5-IP	Tb927.11.14590	70.30	33	51.70	1,627.54
TbEIF4G5	Tb927.8.4500	84.60	52	51.70	7,113.24
TbEIF4E6	Tb927.7.1670	20.90	9	41.40	2,163.60
UMSBP	Tb927.10.6070	14.60	6	37.90	499.91
RBP16	Tb927.11.7900	15.11	7	42.60	496.37
Glyceraldehyde 3-phosphate dehydrogenase	Tb927.6.4280	39.04	9	33.70	487.38
ALBA3	Tb927.4.2040	20.80	8	38.40	460.45
UMSBP	Tb927.10.6060	21.83	8	33.80	451.80
Cyclophilin A	Tb927.11.880	18.71	3	19.20	395.41
Hypothetical protein	Tb927.9.4960	7.60	2	31.20	364.52

[a] GeneDB identifiers are from *T. brucei* 927, version 6.0 (www.genedb.org and www.tritrypdb.org). Temporary GeneDB identifiers retrieved from peptide analysis based on *T. brucei* 927 version 2.2: Tb927.11.14590, Tb11.01.6200; Tb927.11.7900, Tb11.02.5770; Tb927.11.880, Tb11.03.0250; Tb927.9.4960, Tb09.160.3530.
[b] AvUniPepts, number of peptides identified.
[c] NSAF, normalized spectral abundance factor.

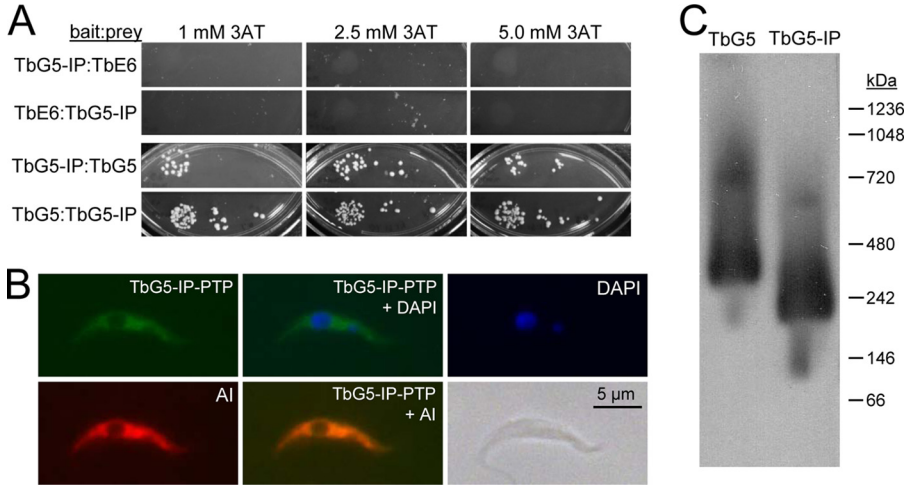

FIG 9 TbG5-IP interacts with the TbE6 complex through direct binding to TbG5 and localizes to the cytosol. A yeast two-hybrid assay tested the interaction potential between TbG5-IP and TbE6 or TbG5 in reciprocal bait and prey orientations. The conditions and interpretation are as noted in the legend to Fig. 6. (B) Localization of TbG5-IP with the TbG5-IP$^{-/PTP}$ cell line and anti-protein A antibody for detection (green). The positive control for cytosolic location was counterstaining with rabbit antibody against the TbEIF4AI protein (red) (51). The negative control is shown in Fig. 3. The outline of the cell is shown in the phase-contrast image. (C) Blue native gel analysis of the TbG5-IP-kDa protein. The TbG5 lane shown for comparison is the same as that shown in Fig. 8.

pression. The *T. brucei* eIF4E family of RNA cap-binding proteins now has two new members, one of which is characterized here and brings the total number of homologs to six. TbE6 is a cytosolic protein that binds RNA cap analogs *in vitro*, specifically, the cap 4 structure carried on the 5′ end of every nucleus-encoded mRNA and on the mature SL RNA *trans*-splicing substrate. The smallest member of the family, TbE6, interacts exclusively with the TbG5 member of the TbEIF4G family, a protein that, in turn, mediates the association of an interesting 70.3-kDa protein named TbG5-IP that shows similarity to two domains associated with RNA cap 0 formation. Knockdown of TbE6 revealed a phenotype consistent with a weakening of the flagellar attachment along the length of the cell body. These compromised cells remain in liquid suspension and appear intact when cultures are not physically manipulated. However, the disturbance associated with centrifugation and pipetting resulted in a high proportion of flagella separating from along the cell body or release altogether, and the ability of TbE6-depleted cells to participate in SoMo behavior on a semisolid surface was reduced. Translation levels were not reduced catastrophically upon TbE6 depletion; thus, the implication of this study is that a subset of proteins associated with maintaining the integrity of flagellar attachment are reduced or missing because of direct or secondary consequences of TbE6 manipulation, a model that we are exploring actively.

A genome-wide RNAi survey performed by Alsford et al. indicated that each of the three members of the TbE6 complex is essential for normal cell growth, with the behavior of TbG5 in differentiating bloodstream forms being the only exception (52). As the level of knockdown achieved in our TbE6 RNAi line allowed cell division approximating that of WT culture, we were afforded a chance to assess the effects of depletion of a key protein. The observed detachment of the flagellum from the length of the cell body resembles that reported following RNAi knockdown of calmodulin (64) and may represent an underlying fault in membrane integrity. Detachment could be elicited in induced cultures in the absence of the fixation step (data not shown) and was dependent on physical manipulation such as centrifugation or vigorous pipetting. The distinction between the maintenance of suspension in liquid media and SoMo behavior may reveal the limit of external stimuli that compromised TbE6-depleted cells can tolerate with respect to the normal integrity and function of their flagellum. If SoMo-level force is required for cell survival in the wild, loss of TbE6 could, like defects in integral flagellum components (65), result in a loss or decrease of parasite virulence.

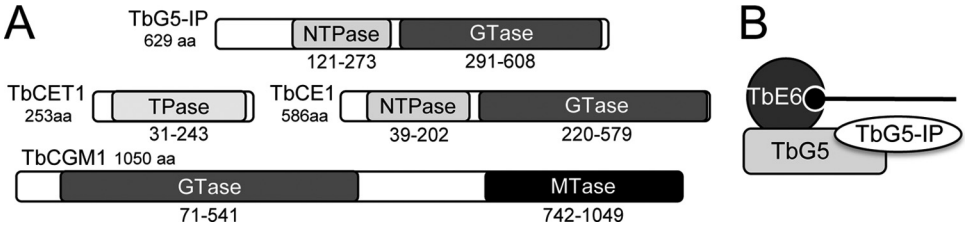

FIG 10 Composition of the TbE6 complex and domains predicted for the TbE6-associated proteins compared to related proteins. (A) Schematic locations of the conserved structural domains in TbG5 and the TbE6-associated mRNA capping enzyme homolog TbG5-IP as predicted by PHYRE^2. The TbCE1 gene lies adjacent to the TbG5-IP gene; TbCET1 and TbCGM1 carry the activities thought to be involved in cap 0 formation on the SL RNA. NTPase, NTP hydrolase; GTase, guanylyltransferase; TPase, triphosphatase; MTase, methyltransferase. (B) The components that copurified with TbE6 are shown, not scaled for size. The RNA (black line; the black circle represents 5′-end cap 4) is recognized by the cap-binding eIF4E component (gray circle). The scaffold protein TbG5 (light gray rectangle) interacts directly with both TbE6 and TbG5-IP.

Whether the defect directly affects a component involved in flagellum attachment, indirectly affects a control step in flagellum structure and maintenance, or represents a nonspecific event is under investigation.

The regulation of subsets of genes at the posttranscriptional level is known to occur in multiple systems but is not well understood mechanistically. Variables such as RNA stability, cytosolic partitioning, or sequestration can come into play, with the key signals carried on the mRNA itself, often in the untranslated region flanking the gene. The mRNA-binding specificity of the TbE6 complex and the catalytic possibilities of TbG5-IP are being examined currently and will provide the best indication of the function of the TbE6 complex. Given the heavy hints provided by the NTP hydrolase and guanylyltransferase domains, mRNA cap modifications are a reasonable assumption if active catalysis by TbG5-IP is involved. If acting on an intact cap 4 structure, removal of cap 0 could serve to destabilize target mRNAs, while previously decapped transcripts might begin their return path to active transcription by passing through this complex. As a precedent, a cytosolic capping activity has been identified in mammalian cells (66). Alternatively, the complex may serve as a selector of mRNAs, constituting a set of coordinated transcripts termed a regulon (67–69), by recognizing specific nucleic acid sequence motifs or structures, presumably through sequences other than the universal SL exon, or perhaps via an RNA-binding protein intermediary.

Our future studies will be directed at determining the enzymatic activity of TbG5-IP, focusing initially on *in vitro* activities on various mRNA cap structures. Concurrently, the identities of the mRNAs associated with the E6-PTP complex and the proteins impacted by E6 knockdown are being explored. We seek to determine what subpopulation of genes is controlled by the TbE6 complex, the molecular signal responsible for conferring specificity, and the specific mechanism that may be repressing the translation of a subset of genes involved in flagellar attachment and possibly other pathways.

ACKNOWLEDGMENTS

This work was supported by a UCLA Stein-Oppenheimer award to D.A.C., NIH awards AI056034 and AI073806 to D.A.C. and N.R.S. and TW009035 to D.A.C. and O.P.D.M.N., NIH award AI052348 to K.H., and NIH award GM089778 to J.A.W. Scholarships for A.M.M. and J.D.F.N. were provided by the Brazilian Funding Agencies FACEPE, CAPES, and CNPq. E.D. and J.Z. were supported by the National Science Center of Poland (UMO-2012/07/B/NZ1/00118 and UMO-2013/08/A/NZ1/00866).

We thank Bidyottam Mittra, Jun Urano, Laurie Read, and Fuyu Tamanoi for strains, reagents, and help with the Y2H assay and Arthur Günzl for the PTP immunofluorescence protocol.

REFERENCES

1. **Berriman M, Ghedin E, Hertz-Fowler C, Blandin G, Renauld H, Bartholomeu DC, Lennard NJ, Caler E, Hamlin NE, Haas B, Bohme U, Hannick L, Aslett MA, Shallom J, Marcello L, Hou L, Wickstead B, Alsmark UC, Arrowsmith C, Atkin RJ, Barron AJ, Bringaud F, Brooks K, Carrington M, Cherevach I, Chillingworth TJ, Churcher C, Clark LN, Corton CH, Cronin A, Davies RM, Doggett J, Djikeng A, Feldblyum T, Field MC, Fraser A, Goodhead I, Hance Z, Harper D, Harris BR, Hauser H, Hostetler J, Ivens A, Jagels K, Johnson D, Johnson J, Jones K, Kerhornou AX, Koo H, Larke N, et al.** 2005. The genome of the African trypanosome *Trypanosoma brucei*. Science **309:**416–422. http://dx.doi.org/10.1126/science.1112642.
2. **Kelly S, Kramer S, Schwede A, Maini PK, Gull K, Carrington M.** 2012. Genome organization is a major component of gene expression control in response to stress and during the cell division cycle in trypanosomes. Open Biol. **2:**120033. http://dx.doi.org/10.1098/rsob.120033.
3. **Clayton C.** 2002. Life without transcriptional control? From fly to man and back again. EMBO J. **21:**1881–1888. http://dx.doi.org/10.1093/emboj/21.8.1881.
4. **Kramer S.** 2012. Developmental regulation of gene expression in the absence of transcriptional control: the case of kinetoplastids. Mol. Biochem. Parasitol. **181:**61–72. http://dx.doi.org/10.1016/j.molbiopara.2011.10.002.
5. **Horn D, McCulloch R.** 2010. Molecular mechanisms underlying the control of antigenic variation in African trypanosomes. Curr. Opin. Microbiol. **13:**700–705. http://dx.doi.org/10.1016/j.mib.2010.08.009.
6. **Rudenko G.** 2010. Epigenetics and transcriptional control in African trypanosomes. Essays Biochem. **48:**201–219. http://dx.doi.org/10.1042/bse0480201.
7. **Liang X-H, Haritan A, Uliel S, Michaeli S.** 2003. *trans* and *cis* splicing in trypanosomatids: mechanisms, factors, and regulation. Eukaryot. Cell **2:**830–840. http://dx.doi.org/10.1128/EC.2.5.830-840.2003.
8. **Sturm NR, Zamudio JR, Campbell DA.** 2012. SL RNA biogenesis in kinetoplastids: a long and winding road, p 29–47. *In* Bindereif A (ed), RNA metabolism in trypanosomes. Springer, Berlin, Germany.
9. **Bangs JD, Crain PF, Hashizume T, McCloskey JA, Boothroyd JC.** 1992. Mass spectrometry of mRNA cap 4 from trypanosomatids reveals two novel nucleosides. J. Biol. Chem. **267:**9805–9815.
10. **Matthews KR, Tschudi C, Ullu E.** 1994. A common pyrimidine-rich motif governs trans-splicing and polyadenylation of tubulin polycistronic pre-mRNA in trypanosomes. Genes Dev. **8:**491–501. http://dx.doi.org/10.1101/gad.8.4.491.
11. **Nilsen TW.** 2001. Evolutionary origin of SL-addition *trans*-splicing: still an enigma. Trends Genet. **17:**678–680. http://dx.doi.org/10.1016/S0168-9525(01)02499-4.
12. **Lasda EL, Blumenthal T.** 2011. *Trans*-splicing. Wiley Interdiscip Rev. RNA **2:**417–434. http://dx.doi.org/10.1002/wrna.71.
13. **Bitar M, Boroni M, Macedo AM, Machado CR, Franco GR.** 2013. The spliced leader trans-splicing mechanism in different organisms: molecular details and possible biological roles. Front. Genet. **4:**199. http://dx.doi.org/10.3389/fgene.2013.00199.
14. **Ghosh A, Lima CD.** 2010. Enzymology of RNA cap synthesis. Wiley Interdiscip. Rev. RNA **1:**152–172. http://dx.doi.org/10.1002/wrna.
15. **Ho CK, Shuman S.** 2001. *Trypanosoma brucei* RNA triphosphatase. J. Biol. Chem. **276:**46182–46186. http://dx.doi.org/10.1074/jbc.M108706200.
16. **Takagi Y, Sindkar S, Ekonomidis D, Hall MP, Ho CK.** 2007. *Trypanosoma brucei* encodes a bifunctional capping enzyme essential for cap 4 formation on the spliced leader RNA. J. Biol. Chem. **282:**15995–16005. http://dx.doi.org/10.1074/jbc.M701569200.
17. **Ruan J-P, Shen S, Ullu E, Tschudi C.** 2007. Evidence for a capping enzyme with specificity for the trypanosome spliced leader RNA. Mol. Biochem. Parasitol. **156:**246–254. http://dx.doi.org/10.1016/j.molbiopara.2007.09.001.
18. **Zamudio JR, Mittra B, Campbell DA, Sturm NR.** 2009. Hypermethylated cap 4 maximizes *Trypanosoma brucei* translation. Mol. Microbiol. **72:**1100–1110. http://dx.doi.org/10.1111/j.1365-2958.2009.06696.x.
19. **Haile S, Papadopoulou B.** 2007. Developmental regulation of gene expression in trypanosomatid parasitic protozoa. Curr. Opin. Microbiol. **10:**569–577. http://dx.doi.org/10.1016/j.mib.2007.10.001.
20. **Richter JD, Sonenberg N.** 2005. Regulation of cap-dependent translation by eIF4E inhibitory proteins. Nature **433:**477–480. http://dx.doi.org/10.1038/nature03205.
21. **Gallie DR, Browning KS.** 2001. eIF4G functionally differs from eIFiso4G in promoting internal initiation, cap-independent translation, and translation of structured mRNAs. J. Biol. Chem. **276:**36951–36960. http://dx.doi.org/10.1074/jbc.M103869200.
22. **Clarkson BK, Gilbert WV, Doudna JA.** 2010. Functional overlap between eIF4G isoforms in *Saccharomyces cerevisiae*. PLoS One **5:**e9114. http://dx.doi.org/10.1371/journal.pone.0009114.
23. **Ptushkina M, Malys N, McCarthy JE.** 2004. eIF4E isoform 2 in *Schizosaccharomyces pombe* is a novel stress-response factor. EMBO Rep. **5:**311–316. http://dx.doi.org/10.1038/sj.embor.7400088.
24. **Keiper BD, Lamphear BJ, Deshpande AM, Jankowska-Anyszka M, Aamodt EJ, Blumenthal T, Rhoads RE.** 2000. Functional characterization of five eIF4E isoforms in *Caenorhabditis elegans*. J. Biol. Chem. **275:**10590–10596. http://dx.doi.org/10.1074/jbc.275.14.10590.
25. **Contreras V, Richardson MA, Hao E, Keiper BD.** 2008. Depletion of the

cap-associated isoform of translation factor eIF4G induces germline apoptosis in C. elegans. Cell Death Differ. **15:**1232–1242. http://dx.doi.org/10.1038/cdd.2008.46.

26. **Yoffe Y, Zuberek J, Lerer A, Lewdorowicz M, Stepinski J, Altmann M, Darzynkiewicz E, Shapira M.** 2006. Binding specificities and potential roles of isoforms of eukaryotic initiation factor eIF4E in *Leishmania*. Eukaryot. Cell **5:**1969–1979. http://dx.doi.org/10.1128/EC.00230-06.
27. **Freire ER, Dhalia R, Moura DM, da Costa Lima TD, Lima RP, Reis CR, Hughes K, Figueiredo RC, Standart N, Carrington M, de Melo Neto OP.** 2011. The four trypanosomatid eIF4E homologues fall into two separate groups, with distinct features in primary sequence and biological properties. Mol. Biochem. Parasitol. **176:**25–36. http://dx.doi.org/10.1016/j.molbiopara.2010.11.011.
28. **Yoffe Y, Léger M, Zinoviev A, Zuberek J, Darzynkiewicz E, Wagner G, Shapira M.** 2009. Evolutionary changes in the *Leishmania* eIF4F complex involve variations in the eIF4E-eIF4G interactions. Nucleic Acids Res. **10:**3243–3253. http://dx.doi.org/10.1093/nar/gkp190.
29. **Zinoviev A, Shapira M.** 2012. Evolutionary conservation and diversification of the translation initiation apparatus in trypanosomatids. Comp. Funct. Genomics **2012:**813718. http://dx.doi.org/10.1155/2012/813718.
30. **Vasquez JJ, Hon CC, Vanselow JT, Schlosser A, Siegel TN.** 2014. Comparative ribosome profiling reveals extensive translational complexity in different *Trypanosoma brucei* life cycle stages. Nucleic Acids Res. **42:**3623–3637. http://dx.doi.org/10.1093/nar/gkt1386.
31. **Hertz-Fowler C, Peacock CS, Wood V, Aslett M, Kerhornou A, Mooney P, Tivey A, Berriman M, Hall N, Rutherford K, Parkhill J, Ivens AC, Rajandream MA, Barrell B.** 2004. GeneDB: a resource for prokaryotic and eukaryotic organisms. Nucleic Acids Res. **32:**D339–D343. http://dx.doi.org/10.1093/nar/gkh007.
32. **Aslett M, Aurrecoechea C, Berriman M, Brestelli J, Brunk BP, Carrington M, Depledge DP, Fischer S, Gajria B, Gao X, Gardner MJ, Gingle A, Grant G, Harb OS, Heiges M, Hertz-Fowler C, Houston R, Innamorato F, Iodice J, Kissinger JC, Kraemer E, Li W, Logan FJ, Miller JA, Mitra S, Myler PJ, Nayak V, Pennington C, Phan I, Pinney DF, Ramasamy G, Rogers MB, Roos DS, Ross C, Sivam D, Smith DF, Srinivasamoorthy G, Stoeckert CJ, Jr, Subramanian S, Thibodeau R, Tivey A, Treatman C, Velarde G, Wang H.** 2010. TriTrypDB: a functional genomic resource for the Trypanosomatidae. Nucleic Acids Res. **38:**D457–D462. http://dx.doi.org/10.1093/nar/gkp851.
33. **Jackson AP, Quail MA, Berriman M.** 2008. Insights into the genome sequence of a free-living Kinetoplastid: *Bodo saltans* (Kinetoplastida: Euglenozoa). BMC Genomics **9:**594. http://dx.doi.org/10.1186/1471-2164-9-594.
34. **Wickstead B, Ersfeld K, Gull K.** 2002. Targeting of a tetracycline-inducible expression system to the transcriptionally silent minichromosomes of Trypanosoma brucei. Mol. Biochem. Parasitol. **125:**211–216. http://dx.doi.org/10.1016/S0166-6851(02)00238-4.
35. **Schimanski B, Nguyen TN, Günzl A.** 2005. Highly efficient tandem affinity purification of trypanosome protein complexes based on a novel epitope combination. Eukaryot. Cell **4:**1942–1950. http://dx.doi.org/10.1128/EC.4.11.1942-1950.2005.
36. **Niedzwiecka A, Marcotrigiano J, Stepinski J, Jankowska-Anyszka M, Wyslouch-Cieszynska A, Dadlez M, Gingras AC, Mak P, Darzynkiewicz E, Sonenberg N, Burley SK, Stolarski R.** 2002. Biophysical studies of eIF4E cap-binding protein: recognition of mRNA 5′ cap structure and synthetic fragments of eIF4G and 4E-BP1 proteins. J. Mol. Biol. **319:**615–635. http://dx.doi.org/10.1016/S0022-2836(02)00328-5.
37. **Cunningham I.** 1977. New culture medium for maintenance of tsetse tissues and growth of trypanosomatids. J. Protozool. **24:**325–329. http://dx.doi.org/10.1111/j.1550-7408.1977.tb00987.x.
38. **Hill KL, Hutchings NR, Russell DG, Donelson JE.** 1999. A novel protein targeting domain directs proteins to the anterior cytoplasmic face of the flagellar pocket in African trypanosomes. J. Cell Sci. **112:**3091–3101.
39. **Oberholzer M, Langousis G, Nguyen HT, Saada EA, Shimogawa MM, Jonsson ZO, Nguyen SM, Wohlschlegel JA, Hill KL.** 2011. Independent analysis of the flagellum surface and matrix proteomes provides insight into flagellum signaling in mammalian-infectious Trypanosoma brucei. Mol. Cell. Proteomics **10:**M111.010538. http://dx.doi.org/10.1074/mcp.M111.010538.
40. **Bastin P, Pullen TJ, Sherwin T, Gull K.** 1999. Protein transport and flagellum assembly dynamics revealed by analysis of the paralysed trypanosome mutant snl-1. J. Cell Sci. **112:**3769–3777.
41. **Oberholzer M, Lopez MA, McLelland BT, Hill KL.** 2010. Social motility in African trypanosomes. PLoS Pathog. **6:**e1000739. http://dx.doi.org/10.1371/journal.ppat.1000739.
42. **Ammerman ML, Downey KM, Hashimi H, Fisk JC, Tomasello DL, Faktorova D, Kafkova L, King T, Lukes J, Read LK.** 2012. Architecture of the trypanosome RNA editing accessory complex, MRB1. Nucleic Acids Res. **40:**5637–5650. http://dx.doi.org/10.1093/nar/gks211.
43. **Schägger H, von Jagow G.** 1991. Blue native electrophoresis for isolation of membrane protein complexes in enzymatically active form. Anal. Biochem. **199:**223–231. http://dx.doi.org/10.1016/0003-2697(91)90094-A.
44. **Zamudio JR, Mittra B, Chattopadhyay A, Wohlschlegel JA, Sturm NR, Campbell DA.** 2009. *Trypanosoma brucei* spliced leader RNA maturation by the cap 1 2′-*O*-ribose methyltransferase and SLA1 H/ACA snoRNA pseudouridine synthase complex. Mol. Cell. Biol. **29:**1202–1211. http://dx.doi.org/10.1128/MCB.01496-08.
45. **Peng J, Elias JE, Thoreen CC, Licklider LJ, Gygi SP.** 2002. Evaluation of multidimensional chromatography coupled with tandem mass spectrometry (LC/LC-MS/MS) for large-scale protein analysis: the yeast proteome. J. Proteome Res. **2:**43–50. http://dx.doi.org/10.1021/pr025556v.
46. **Haghighat A, Sonenberg N.** 1997. eIF4G dramatically enhances the binding of eIF4E to the mRNA 5′-cap structure. J. Biol. Chem. **272:**21677–21680. http://dx.doi.org/10.1074/jbc.272.35.21677.
47. **von Der Haar T, Ball PD, McCarthy JE.** 2000. Stabilization of eukaryotic initiation factor 4E binding to the mRNA 5′-Cap by domains of eIF4G. J. Biol. Chem. **275:**30551–30555. http://dx.doi.org/10.1074/jbc.M004565200.
48. **Kaye NM, Emmett KJ, Merrick WC, Jankowsky E.** 2009. Intrinsic RNA binding by the eukaryotic initiation factor 4F depends on a minimal RNA length but not on the m7G cap. J. Biol. Chem. **284:**17742–17750. http://dx.doi.org/10.1074/jbc.M109.009001.
49. **Yanagiya A, Svitkin YV, Shibata S, Mikami S, Imataka H, Sonenberg N.** 2009. Requirement of RNA binding of mammalian eukaryotic translation initiation factor 4GI (eIF4GI) for efficient interaction of eIF4E with the mRNA cap. Mol. Cell. Biol. **29:**1661–1669. http://dx.doi.org/10.1128/MCB.01187-08.
50. **Kramer S, Queiroz R, Ellis L, Webb H, Hoheisel JD, Clayton C, Carrington M.** 2008. Heat shock causes a decrease in polysomes and the appearance of stress granules in trypanosomes independently of eIF2α phosphorylation at Thr169. J. Cell Sci. **121:**3002–3014. http://dx.doi.org/10.1242/jcs.031823.
51. **Dhalia R, Marinsek N, Reis CR, Katz R, Muniz JR, Standart N, Carrington M, de Melo Neto OP.** 2006. The two eIF4A helicases in *Trypanosoma brucei* are functionally distinct. Nucleic Acids Res. **34:**2495–2507. http://dx.doi.org/10.1093/nar/gkl290.
52. **Alsford S, Turner DJ, Obado SO, Sanchez-Flores A, Glover L, Berriman M, Hertz-Fowler C, Horn D.** 2011. High-throughput phenotyping using parallel sequencing of RNA interference targets in the African trypanosome. Genome Res. **21:**915–924. http://dx.doi.org/10.1101/gr.115089.110.
53. **Kim HS, Li Z, Boothroyd C, Cross GA.** 2013. Strategies to construct null and conditional null *Trypanosoma brucei* mutants using Cre-recombinase and loxP. Mol. Biochem. Parasitol. **191:**16–19. http://dx.doi.org/10.1016/j.molbiopara.2013.08.001.
54. **Merritt C, Stuart K.** 2013. Identification of essential and non-essential protein kinases by a fusion PCR method for efficient production of transgenic *Trypanosoma brucei*. Mol. Biochem. Parasitol. **190:**44–49. http://dx.doi.org/10.1016/j.molbiopara.2013.05.002.
55. **Park SH, Nguyen BN, Kirkham JK, Nguyen TN, Gunzl A.** 11 April 2014. A new strategy of RNA interference that targets heterologous sequences reveals CITFA1 as an essential component of class I transcription factor A in *Trypanosoma brucei*. Eukaryot. Cell http://dx.doi.org/10.1128/EC.00014-14.
56. **Gingras AC, Raught B, Sonenberg N.** 1999. eIF4 initiation factors: effectors of mRNA recruitment to ribosomes and regulators of translation. Annu. Rev. Biochem. **68:**913–963. http://dx.doi.org/10.1146/annurev.biochem.68.1.913.
57. **Zinoviev A, Leger M, Wagner G, Shapira M.** 2011. A novel 4E-interacting protein in Leishmania is involved in stage-specific translation pathways. Nucleic Acids Res. **39:**8404–8415. http://dx.doi.org/10.1093/nar/gkr555.
58. **Marintchev A, Wagner G.** 2005. eIF4G and CBP80 share a common origin and similar domain organization: implications for the structure and function of eIF4G. Biochemistry **44:**12265–12272. http://dx.doi.org/10.1021/bi051271v.
59. **Li H, Tschudi C.** 2005. Novel and essential subunits in the 300-kilodalton

nuclear cap binding complex of *Trypanosoma brucei*. Mol. Cell. Biol. **25:** 2216–2226. http://dx.doi.org/10.1128/MCB.25.6.2216-2226.2005.
60. **Barbosa I, Haque N, Fiorini F, Barrandon C, Tomasetto C, Blanchette M, Le Hir H.** 2012. Human CWC22 escorts the helicase eIF4AIII to spliceosomes and promotes exon junction complex assembly. Nat. Struct. Mol. Biol. **19:**983–990. http://dx.doi.org/10.1038/nsmb.2380.
61. **Virgili G, Frank F, Feoktistova K, Sawicki M, Sonenberg N, Fraser CS, Nagar B.** 2013. Structural analysis of the DAP5 MIF4G domain and its interaction with eIF4A. Structure **21:**517–527. http://dx.doi.org/10.1016/j.str.2013.01.015.
62. **Kelley LA, Sternberg MJ.** 2009. Protein structure prediction on the Web: a case study using the Phyre server. Nat. Protoc. **4:**363–371. http://dx.doi.org/10.1038/nprot.2009.2.
63. **Silva E, Ullu E, Kobayashi R, Tschudi C.** 1998. Trypanosome capping enzymes display a novel two-domain structure. Mol. Cell. Biol. **18:**4612–4619.
64. **Ginger ML, Collingridge PW, Brown RW, Sproat R, Shaw MK, Gull K.** 2013. Calmodulin is required for paraflagellar rod assembly and flagellum-cell body attachment in trypanosomes. Protist **164:**528–540. http://dx.doi.org/10.1016/j.protis.2013.05.002.
65. **Kisalu NK, Langousis G, Bentolila LA, Ralston KS, Hill KL.** 2014. Mouse infection and pathogenesis by *Trypanosoma brucei* motility mutants. Cell Microbiol. **16:**912–924. http://dx.doi.org/10.1111/cmi.12244.
66. **Otsuka Y, Kedersha NL, Schoenberg DR.** 2009. Identification of a cytoplasmic complex that adds a cap onto 5′-monophosphate RNA. Mol. Cell. Biol. **29:**2155–2167. http://dx.doi.org/10.1128/MCB.01325-08.
67. **Culjkovic B, Topisirovic I, Skrabanek L, Ruiz-Gutierrez M, Borden KL.** 2006. eIF4E is a central node of an RNA regulon that governs cellular proliferation. J. Cell Biol. **175:**415–426. http://dx.doi.org/10.1083/jcb.200607020.
68. **Keene JD.** 2007. RNA regulons: coordination of post-transcriptional events. Nat. Rev. Genet. **8:**533–543. http://dx.doi.org/10.1038/nrg2111.
69. **Ouellette M, Papadopoulou B.** 2009. Coordinated gene expression by post-transcriptional regulons in African trypanosomes. J. Biol. **8:**100. http://dx.doi.org/10.1186/jbiol203.
70. **Landsman D, Bustin M.** 1993. A signature for the HMG-1 box DNA-binding proteins. Bioessays **15:**539–546. http://dx.doi.org/10.1002/bies.950150807.
71. **Marcotrigiano J, Lomakin IB, Sonenberg N, Pestova TV, Hellen CU, Burley SK.** 2001. A conserved HEAT domain within eIF4G directs assembly of the translation initiation machinery. Mol. Cell **7:**193–203. http://dx.doi.org/10.1016/S1097-2765(01)00167-8.